

# Continuous-Variable Entangled States of Light carrying Orbital Angular Momentum

A. Pecoraro<sup>1,2</sup>, F. Cardano<sup>2</sup>, L. Marrucci<sup>2</sup> and A. Porzio<sup>1a</sup>

<sup>1</sup> *SPIN – CNR, Napoli, Complesso Universitario di Monte Sant’Angelo,  
via Cintia, 80126 Napoli, Italy and*

<sup>2</sup> *Dipartimento di Fisica, Universitá ”Federico II”, via Cintia, 80126 Napoli, Italy*

(Dated: December 3, 2024)

## Abstract

The orbital angular momentum of light, unlike spin, is an infinite-dimensional discrete variable and may hence offer enhanced performances for encoding, transmitting, and processing information in the quantum regime. Hitherto, this degree of freedom of light has been studied mainly in the context of quantum states with definite number of photons. On the other hand, field-quadrature continuous-variable quantum states of light allow implementing many important quantum protocols not accessible with photon-number states. Here, we present the first generation and complete experimental characterization of a bipartite continuous-variable Gaussian entangled state endowed with non-zero orbital angular momentum. A q-plate is used to transfer the continuous-variable entanglement initially generated in polarization into orbital angular momentum. We then apply a reconfigurable homodyne detector to various combinations of orbital angular momentum modes in order to reconstruct the entire quantum-state covariance matrix, by directly measuring the fluctuations of quadrature operators. Our work is a step towards generating multipartite continuous-variable entanglement in a single optical beam.

PACS numbers: 03.67.Bg Entanglement production and manipulation; 42.50.Tx Optical angular momentum and its quantum aspects; 42.50.Dv Quantum state engineering and measurements;

---

<sup>a</sup> Corresponding author: alberto.porzio@spin.cnr.it

Accessing high-dimensional effective Hilbert spaces is crucial for implementing complex quantum information (QI) tasks. The continuous-variable (CV) encoding provides a convenient possible approach to this purpose, as it spans an inherently infinite Hilbert space and it naturally allows quantum communication and processing with larger alphabets [1, 2]. This approach is often investigated within quantum optical platforms, by using optical field quadratures as the variables.

Gaussian bipartite entanglement in optical CV QI is commonly generated by means of below-threshold optical parametric oscillators (OPOs), which exploit either spatial separation or polarization, i.e. spin angular momentum (SAM), as distinguishing (or “label”) degree-of-freedom (d.o.f.) [3–6]. It would be, however, highly desirable to move towards CV *multipartite* entanglement. This goal could be possibly sought by introducing additional discrete degrees of freedom with which labelling CVs, that is by adopting what can be termed a “hybrid discrete-continuous variable” strategy to carrying out QI. Eventually, a single degree of freedom can be exploited, in case it is associated with multiple orthogonal modes. These approaches may also lead to other interesting outcomes, such as CV hyper-entanglement [7].

A possible route for implementing such a strategy is by using transverse modes of a single optical beam as additional discrete-variable d.o.f. Transverse optical modes, and in particular those carrying orbital angular momentum (OAM), have been the subject of much research in quantum optics, recently. In particular, OAM can conveniently provide a large set of orthogonal modes within a single optical beam, as demonstrated in a number of experiments in which high-dimensional Hilbert spaces and entanglement have been achieved [9]. However, this research focused mainly on “digital” photon-number quantum optics [10, 11], while not much has been done hitherto by combining CV quantum optics and OAM.

An indirect proof of Gaussian CV entanglement between OAM modes has been first reported by Lassen *et al.* [12], specifically by showing quantum squeezing of a first-order Hermite-Gaussian (HG) mode that corresponds to a balanced superposition of two opposite-OAM ( $\pm 1$ ) Laguerre-Gaussian (LG) modes. A similar approach, i.e. the measurement of quadrature-squeezing of first-order HG modes, has been adopted by Liu *et al.* [8] to demonstrate experimentally the first hyper-entangled CV state. However, both these works demonstrated directly only the squeezing of the OAM-superposition HG modes. A complete characterization of OAM-mode CV entanglement, that for Gaussian states amounts

to measuring the full covariance matrix of the two entangled modes [13], has been hitherto missing.

In the work reported here, we endow a pair of cross-polarized CV entangled modes with non-zero OAM, thus realising multi-d.o.f. CV entanglement with the two entangled modes labelled by both SAM and OAM. Then, we use a novel spatial-mode-reconfigurable homodyne detector [14] to measure directly the quadratures of various linear combinations of the two entangled CVs, thus enabling us to reconstruct their full covariance matrix (CM). In this way, we provide what is the first complete characterization of such a SAM-OAM CV entanglement, to our knowledge.

Optical beams for which photons carry a definite amount of OAM correspond to the so-called “helical modes” of light, i.e. paraxial light beams characterized by a helical phase factor  $e^{im\varphi}$  where  $\varphi$  is the azimuthal angle around the propagation axis  $z$  and  $m$  is an integer. An optical vortex with topological charge  $m$  is then present on axis, where the phase is undefined and the light intensity vanishes (doughnut beams) [15, 16]. In these modes, the ratio between OAM and energy fluxes along the optical axis is  $m/\omega$ , where  $\omega$  is the laser frequency. In other words, each photon within the beam carries  $m\hbar$  of OAM along the propagation direction. Quantum states  $|m\rangle$ , describing individual photons whose spatial structure is that of an helical mode, are orthogonal and span an infinite-dimensional Hilbert space.

In our experiment (see Fig. 1 for the setup layout and some technical details), the initial quantum source is a standard type-II phase-matching OPO generating Gaussian bipartite entangled states [17]. The phase matching is adjusted to a degenerate condition [18], so that the two beams have the same frequency, corresponding to a wavelength of 1064 nm. The entangled modes emerge from the OPO as two cross-linearly-polarized continuous-wave (CW) co-propagating beams, both having a Gaussian transverse profile ( $\text{TEM}_{00}$ ), i.e. with vanishing OAM. Let us label as  $H$  ( $V$ ) the horizontal (vertical) linear polarization of the modes generated by the OPO.

OAM is imparted to the two modes generated by the OPO by using a device commonly known as “ $q$ -plate” (qP) [19]. Essentially, a  $q$ -plate is a thin layer of birefringent liquid crystal, sandwiched between containing glasses, and whose optic axis is structured into a singular pattern with topological charge  $q$ , the latter being an integer or half-integer number. The total birefringent phase retardation  $\delta$  can be controlled electrically [20]. Using

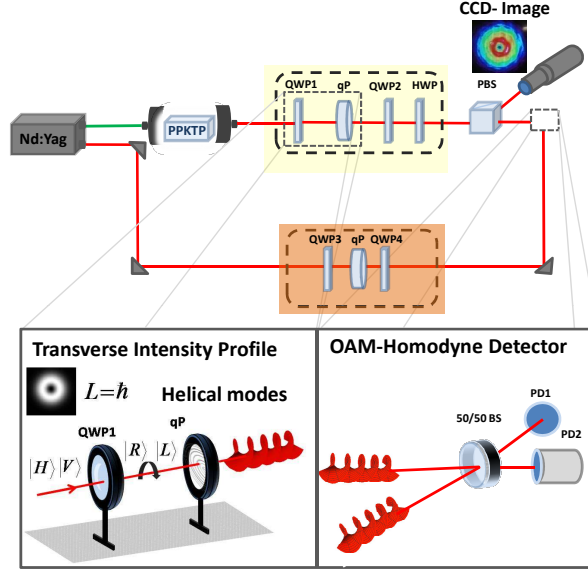


FIG. 1. Schematic of the experimental set-up. A Nd:Yag laser emitting at 1064 nm, internally frequency doubled, acts as pump for an OPO based on a  $\alpha$ -cut PPKTP type-II crystal that generates a pair of frequency-degenerate orthogonally-polarized modes. The OPO [18] oscillation threshold is  $\approx 70$  mW and it is operated at  $\approx 70\%$  of the threshold value. The yellow shadowed area (enlarged in the bottom-left inset) including two quarter-wave plates (QWP1 and QWP2), a  $q$ -plate (qP) and a half-wave plate (HWP), represents the optical set-up for manipulating the SAM and OAM d.o.f. of the entangled beam. A similar set of optical components is placed along the LO path for effective OAM homodyning (dark orange shadow). The bottom-right inset shows an enlarged view of the homodyne detector.

a quantum notation, the optical action of a  $q$ -plate can be simply described by an operator  $\hat{Q}$  defined as follows:

$$\begin{aligned}\hat{Q} |L, m\rangle &= \cos \frac{\delta}{2} |L, m\rangle + i \sin \frac{\delta}{2} |R, m + 2q\rangle \\ \hat{Q} |R, m\rangle &= \cos \frac{\delta}{2} |R, m\rangle + i \sin \frac{\delta}{2} |L, m - 2q\rangle\end{aligned}\quad (1)$$

where  $|A, m\rangle$  denotes a beam with OAM  $m$  and polarization  $A = L, R$ , with  $L$  ( $R$ ) standing for left (right) circular polarization. The radial structure of the beam is also affected by the qP, but we omit it in our notation for brevity (with the understanding that all modes having the same  $|m|$  also have the same radial structure). From Eq. (1) it is seen that a qP couples circular polarization with OAM: for the optimal retardation  $\delta = \pi$ , a single circularly polarized beam passing through the qP reverses its polarization and acquires  $\pm 2q$

quanta of OAM. In our experiment we wish to use the same qP for both beams generated by the OPO, which have orthogonal linear polarizations. Therefore, we first transform these two linear polarizations into circular, by using a quarter-wave plate (QWP1, in Fig. 1) aligned at  $45^\circ$  from the  $H/V$  basis. The QWP1 provides the transformations  $|V\rangle \xrightarrow{\text{QWP1}} |L\rangle$  and  $|H\rangle \xrightarrow{\text{QWP1}} |R\rangle$  (with no OAM variation). Next, the cross-polarized pair of CV entangled beams, now having opposite circular polarizations, pass through the qP, thus inverting their polarization handedness and simultaneously acquiring opposite OAM values (see the bottom-left inset in Fig. 1). In our experiment the qP has  $q = 1/2$ , so that the acquired OAM is given by  $m = \pm 1$ . At the output of the qP, the two entangled modes are still co-propagating and can now be distinguished both by polarization ( $L/R$ ) and OAM ( $\pm 1$ ).

Let us now discuss the quantum fluctuation/correlation properties of these two modes. A sub-threshold OPO is known to generate a pair of modes in a Gaussian quantum state (GS) [13]. The quantum properties of such two-mode GS are described by the canonical field quadrature operators  $R = (X_a, Y_a, X_b, Y_b)$ , where the subscripts  $a$  and  $b$  label the two modes and  $X_k$  and  $Y_k$  are respectively the amplitude and phase quadratures, i.e.  $X_k = (\hat{a}_k + \hat{a}_k^\dagger)/\sqrt{2}$  and  $Y_k = (\hat{a}_k - \hat{a}_k^\dagger)/(i\sqrt{2})$ , where  $\hat{a}_k$  ( $\hat{a}_k^\dagger$ ) denotes the annihilation (creation) operator. The GS itself is completely characterized by the vector of mean values of these quadrature operators and, most importantly, by their CM. The CM  $\sigma$  of a bipartite GS is a real symmetric and positive-definite  $4 \times 4$  matrix whose elements are defined as  $\sigma_{ij} = \frac{1}{2} \langle \{R_i, R_j\} \rangle - \langle R_i \rangle \langle R_j \rangle$ , with  $\{h, g\} = hg + gh$  being the anti-commutator. A sub-threshold type-II OPO, owing to the symmetry of its Hamiltonian, can only produce states whose CM is in the so called standard form [21]:

$$\sigma_S = \begin{pmatrix} n & 0 & c_1 & 0 \\ 0 & n & 0 & c_2 \\ c_1 & 0 & m & 0 \\ 0 & c_2 & 0 & m \end{pmatrix}. \quad (2)$$

where  $n, m$  are physically related to the average photon number of the single entangled mode, and  $c_1$  and  $c_2$  are related to the strength of the quantum correlations. All the relevant criteria for classifying the bipartite-state quantum properties can be written in terms of the CM elements [21], so that its knowledge allows deducing information about the separability or entanglement of the state.

Let us now label the pair of modes at the OPO output as  $(a, b)$  [6]. The initial two-mode quantum state is  $HV$  polarized and has vanishing OAM, so it can be denoted as  $|V, 0\rangle_a |H, 0\rangle_b$ . The GS fluctuation properties (as given by the CM) are known to be preserved under linear optical transformations. Therefore, the action of the QWP1 and qP yields the following transformation:

$$|V, 0\rangle_a |H, 0\rangle_b \xrightarrow{\text{QWP1+qP}} |R, 1\rangle_a |L, -1\rangle_b. \quad (3)$$

At this stage, the resulting bipartite state has acquired an additional d.o.f. for distinguishing the two sub-systems  $a$  and  $b$ , namely OAM, in addition to polarization (or spin). Hence, if the two modes are generated in an entangled state, this now involves correlated fluctuations of both polarization and OAM.

In order to experimentally characterize the quantum properties of this multi-distinguishable CV entangled pair, we wish to apply the single homodyne scheme discussed in Ref. [22]. This, in turn, requires to homodyne modes  $a, b$  as well as the following auxiliary linear-combination modes:

$$\begin{aligned} c &= \frac{a+b}{\sqrt{2}} & d &= \frac{a-b}{\sqrt{2}} \\ e &= \frac{ia+b}{\sqrt{2}} & f &= \frac{ia-b}{\sqrt{2}} \end{aligned} \quad (4)$$

In Ref. [6], these auxiliary modes could be easily obtained from the  $(a, b)$  pair by combination of wave-plates and polarizing beam-splitters (also exploiting the frequency-degeneracy of the two modes). However, we now have the additional OAM d.o.f. and the two modes  $a$  and  $b$  have opposite values of OAM, which makes the task of creating their linear combinations much harder. To overcome this problem, we exploit the qP polarization-control properties for generating the auxiliary modes  $c, d, e$ , and  $f$  directly at the output of the qP (see Fig. 1). First, by turning the QWP1 so that its fast/slow axes coincide with  $H/V$ , we have  $|H\rangle \xrightarrow{\text{QWP1}} |H\rangle$  and  $|V\rangle \xrightarrow{\text{QWP1}} i|V\rangle$ . At the qP output we then obtain

$$\begin{aligned} |H, 0\rangle_a &= \frac{|L, 0\rangle_a + |R, 0\rangle_a}{\sqrt{2}} \xrightarrow{\text{qP}} i \frac{|L, -1\rangle_a - |R, 1\rangle_a}{\sqrt{2}} \\ i|V, 0\rangle_b &= -\frac{|L, 0\rangle_b - |R, 0\rangle_b}{\sqrt{2}} \xrightarrow{\text{qP}} -i \frac{|L, -1\rangle_b + |R, 1\rangle_b}{\sqrt{2}} \end{aligned} \quad (5)$$

Then, grouping for the same polarization and OAM state, we obtain  $|R, 1\rangle_{-i\frac{a+b}{\sqrt{2}}} = -i|R, 1\rangle_c$  and  $|L, -1\rangle_{i\frac{a-b}{\sqrt{2}}} = i|L, -1\rangle_d$ . Hence, up to a global phase, we obtain the  $c$  and  $d$  modes

assigned to two opposite OAM modes and circular polarizations. Similarly, by removing the QWP1 altogether, so that the  $H/V$  linear-polarized entangled modes enter directly the qP, we obtain

$$\begin{aligned} |H, 0\rangle_a &= \frac{|L, 0\rangle_a + |R, 0\rangle_a}{\sqrt{2}} \xrightarrow{\text{qP}} i \frac{|L, -1\rangle_a - |R, 1\rangle_a}{\sqrt{2}} \\ |V, 0\rangle_b &= i \frac{|L, 0\rangle_b - |R, 0\rangle_b}{\sqrt{2}} \xrightarrow{\text{qP}} - \frac{|L, -1\rangle_b + |R, 1\rangle_b}{\sqrt{2}}. \end{aligned} \quad (6)$$

Hence, at the qP output we now have  $|R, 1\rangle_{-\frac{ia+b}{\sqrt{2}}} = |R, 1\rangle_e$  and  $|L, -1\rangle_{\frac{ia-b}{\sqrt{2}}} = |L, -1\rangle_f$ . i.e., modes  $e$  and  $f$ , again in the circular polarization basis and with opposite OAM (see Eq. 4).

The characterization scheme requires to homodyne these six modes. A homodyne detector relies on the interference of the optical signal under scrutiny with a strong (coherent) local oscillator (LO). Thus we have designed a LO branch that generates a coherent optical field in the  $|H, \pm 1\rangle$  mode, i.e. with a nonzero OAM  $\pm 1$ . The homodyne interference is therefore designed, for the first time to our knowledge, to take place directly in the OAM state. The  $H$  polarization of the LO is selected because it is the working polarization of the homodyne beamsplitter (BS) [14]. Before the homodyne interference, a second QWP (QWP2 in Fig. 1) is hence used to revert the polarization state of any mode pair to be characterized to the  $H/V$  basis, while leaving the OAM unchanged. QWP2 is oriented so that  $(|R, 1\rangle, |L, -1\rangle) \xrightarrow{\text{QWP2}} (|V, 1\rangle, |H, -1\rangle)$ . A final half-wave plate (HWP) and a polarizing beam splitter (PBS) in front of the homodyne BS allows one to select which of the modes effectively reaches the detection stage (see Fig. 1). A similar set-up, composed of two QWPs (QWP3 and QWP4 in Fig. 1) and a second qP tailors the LO to the desired  $|H, \pm 1\rangle$  state. The homodyne visibility routinely obtained is  $0.97 \pm 0.01$  [14].

We stress that the above-sketched method is used to measure the quantum correlation of entangled states spanning both polarization and OAM d.o.f.. Indeed, the homodyne selects a given OAM value and a specific polarization state. If quantum correlations did not affect one of the two d.o.f., the measured matrix would not witness any entanglement.

The overall detection efficiency includes photodiodes' quantum efficiency, homodyne visibility, and losses at the photodiodes uncoated windows. The total collection efficiency has to take into account also the cavity output coupling and the qP transmission. All these factors lead to an overall collection efficiency of  $0.52 \pm 0.03$ .

Experimentally we have acquired quadrature traces for the six modes ( $a, b, c, d, e, f$ ). Data have been analysed as in Ref. [21] by a home-made software that extracts all the relevant

values to retrieve the state CM. A typical obtained experimental covariance matrix is

$$\begin{pmatrix} 0.61 \pm 0.02 & 0.00(4) \pm 0.02 & 0.29 \pm 0.02 & -0.01 \pm 0.02 \\ 0.00(4) \pm 0.02 & 0.61 \pm 0.02 & 0.00(5) \pm 0.02 & -0.23 \pm 0.02 \\ 0.29 \pm 0.02 & 0.00(5) \pm 0.02 & 0.60 \pm 0.02 & 0.00(2) \pm 0.02 \\ -0.01 \pm 0.02 & -0.23 \pm 0.02 & 0.00(2) \pm 0.02 & 0.60 \pm 0.02 \end{pmatrix}, \quad (7)$$

in which all elements consistent with zero are reported with the highest significant digit given in parentheses. This matrix is consistent with a quantum state that has suffered 47% of losses [21], in very good agreement with the  $0.52 \pm 0.01$  estimated collection efficiency of the detection set-up. The same matrix is graphically reported in Fig. 2.

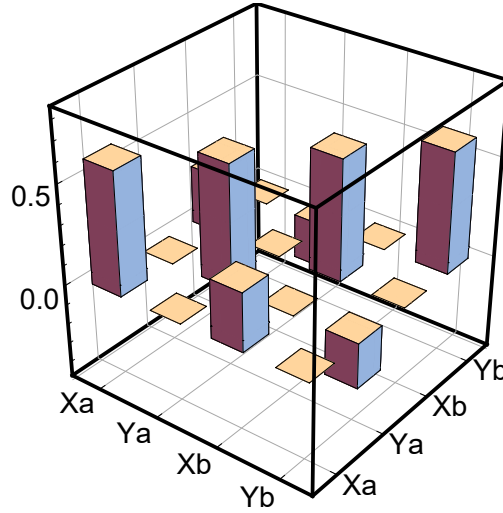


FIG. 2. Graphic representation of the covariance matrix given in Eq. (7). The non-zero elements outside the main diagonal are a signature of quantum correlation between pairs of quadratures of modes carrying different OAM.

In order to prove that this matrix witnesses genuine quantum correlations and represents an entangled CV bipartite Gaussian state we used the Peres-Horodecki-Simon (PHS) [23–25] and the Duan [26] unseparability criteria. Translated into the CM language (see Eq. (2)), the first criterion states that a bipartite Gaussian state is separable if

$$n^2 + m^2 + 2|c_1 c_2| - 4(nm - c_1^2)(nm - c_2^2) \leq \frac{1}{4} \quad (8)$$

and it is entangled otherwise. For the measured matrix in Eq. (7), the left-hand-side of the above inequality is  $0.51 \pm 0.03$ , hence the measured state is entangled with a high statistical

significance ( $> 8\sigma$ ). This can be also confirmed by the Duan criterion [26]. For a CM in the usual standard form, it reads:

$$\sqrt{(2n-1)(2m-1)} - (c_1 - c_2) \geq 0. \quad (9)$$

The state is separable if and only if its CM fulfils the above inequality. The matrix given in Eq. (7) is again found to be unseparable, being the left-hand-side equal to  $-0.31 \pm 0.04$ .

From the measured CM, it is also possible to retrieve the joint photon number probability  $p(n; m)$  of the pure state generated in the crystal [13, 27]. It represents the probability of having exactly  $m$  photons in mode  $b$  and  $n$  photons in mode  $a$ . In Fig. 3, we report the 3D histogram of  $p(n; m)$  for the pure state generated by the non-linear process in the crystal. For a pure two-modes squeezed state, only diagonal terms are non zero. This is a clear signature that the system is in a *twin-beam* state: every time a photon populates mode  $a$  a twin one is certainly in mode  $b$ .

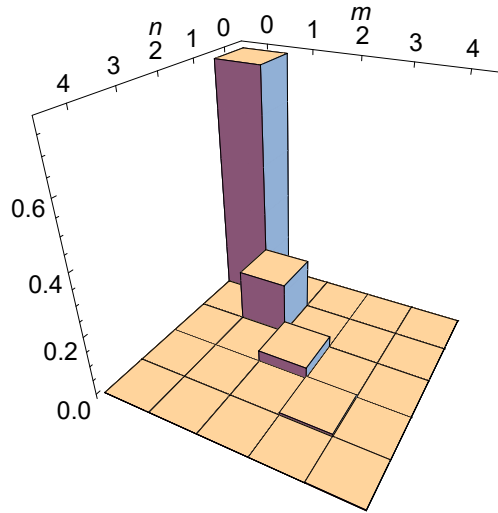


FIG. 3. Joint photon number probability distribution  $p(n; m)$  of the pure *twin-beam* state generated inside the crystal. This state propagates all the way down to the homodyne detector and, after collection and detection losses, is represented by the CM given by Eq. (7).

In conclusion, we have demonstrated the generation and complete experimental characterization of a bipartite continuous-variable entangled state endowed with non-zero OAM. In particular, we have completed the first experimental derivation of the full covariance matrix of the two helical modes, via measurement of the quadrature field correlations of various linear combinations of the generated modes. Although the experiment reported here

concerns bipartite systems, the use of OAM has the potential for generating multipartite quantum states exploiting a hybrid discrete-continuous variable encoding, all within a single optical beam. This, in turn, could for example enable the multiplexing of multiple correlated quantum channels within a single optical channel.

## ACKNOWLEDGEMENT

The authors thank S. Olivares and B. Piccirillo for granting the use of the  $\textcircled{C}$ Mathematica routine for retrieving the joint photon number probability distribution and for the preparation of the *q-plates* used in the experiment, respectively.

## REFERENCES

---

- [1] Frédéric Grosshans and Philippe Grangier, Phys. Rev. Lett. **88**:057902 (2002);
- [2] Frédéric Grosshans, Gilles Van Assche, Jérôme Wenger, Rosa Brouri, Nicolas J. Cerf, and Philippe Grangier, Nature **421**:238 (2003);
- [3] Z. Y. Ou, S. F. Pereira, H. J. Kimble, and K. C. Peng, Phys. Rev. Lett. **68**:3663 (1992);
- [4] W. P. Bowen et al., Phys. Rev. A **69**:012304 (2004);
- [5] Julien Laurat, Gaëlle Keller, José Augusto Oliveira-Huguenin, Claude Fabre, Thomas Coudreau, Alessio Serafini, Gerardo Adesso and Fabrizio Illuminati J. Opt. B **7**:S577 (2005);
- [6] V. D'Auria, S. Fornaro, A. Porzio, S. Solimeno, S. Olivares, and M. G. A. Paris, Phys. Rev. Lett. **102**:020502 (2009);
- [7] B. dos Santos, K. Dechoum, and A. Khoury, Phys. Rev. Lett. **103**:230503 (2009);
- [8] Kui Liu, Jun Guo, Chunxiao Cai, Shuaifeng Guo, and Jiangrui Gao, Phys. Rev. Lett. **113**:170501 (2014);
- [9] Manuel Erhard, Robert Fickler, Mario Krenn, Anton Zeilinger, Light: Science & Applications **7**:17146 (2018);
- [10] Halina Rubinsztein-Dunlop1, Andrew Forbes, M V Berry, M R Dennis, David L Andrews, Masud Mansuripur, Cornelia Denz, Christina Alpmann, Peter Banzer, Thomas Bauer *et al.*

J. Opt. **19**:013001 (2017);

- [11] Amin Babazadeh, Manuel Erhard, Feiran Wang, Mehul Malik, Rahman Nouroozi, Mario Krenn, and Anton Zeilinger Phys Rev Lett **119**:180510 (2017); M. Malik, M. Erhard, M. Huber, M. Krenn, R. Fickler, and A. Zeilinger Nat Photonics **10**:248 (2017);
- [12] M. Lassen, G. Leuchs, and U.L. Andersen, Phys. Rev. Lett. **102**:163602 (2009);
- [13] S. Olivares, The European Physical Journal Special Topics, **203**:3 (2012);
- [14] Adriana Pecoraro *et al.* "Reconfigurable homodyne detector for vortex beams" *in preparation*;
- [15] A. M. Yao and M.J. Padgett Adv. Opt. Photonics **3**:161 (2011);
- [16] M.J. Padgett Opt. Express **25**:11265 (2017);
- [17] Alberto Porzio, Virginia D'Auria, Salvatore Solimeno, Stefano Olivares and Matteo G.A: Paris, Int. J. Quantum Inf. **5**:63 (2007);
- [18] V. D'Auria, S. Fornaro, A. Porzio, E.A. Sete, and S. Solimeno. Applied Physics B, **91**:309, (2008);
- [19] L. Marrucci, C. Manzo, and D. Paparo, Phys. Rev. Lett. **96**:163905 (2006);
- [20] B. Piccirillo, V. DAmbrosio, S. Slussarenko, L. Marrucci, and E. Santamato, Appl. Phys. Lett. **97**:241104 (2010);
- [21] D. Buono, G. Nocerino, A. Porzio, and S. Solimeno. Phys. Rev. A, **86**:042308, (2012);
- [22] Virginia D'Auria, Alberto Porzio, Salvatore Solimeno, Stefano Olivares and Matteo G A Paris, J. Opt. B: Quantum Semiclass. Opt. **7**:S750 (2005);
- [23] Asher Peres Phys. Rev. Lett. **77**:1413 Published 19 August 1996
- [24] Paweł Horodecki, Physics Letters A, **232**:333 (1997);
- [25] R. Simon, Phys. Rev. Lett., **84**:2726 (2000);
- [26] Lu-Ming Duan, G. Giedke, J. I. Cirac, and P. Zoller. Phys. Rev. Lett., **84**:2722 (2000);
- [27] D. Buono, G. Nocerino, V. D'Auria, A. Porzio, S. Olivares, and M. G. A. Paris, J. Opt. Soc. Am. B, **27**:A110 (2010).